Exotic features in the lattice dynamics of an incommensurate overlayer/substrate structure as modeled via the Frenkel-Kontorova system

N. S. Luo, S. Y. Wu, and C. S. Jayanthi
Department of Physics, University of Louisville, Louisville, Kentucky 40292
(Received 28 October 1996)

Using a numerically determined ground state of the infinite Frenkel-Kontorova chain and the method of real-space Green's function, we have calculated the phonon dispersion curve of the incommensurate phase of this system. The phonon frequency spectrum exhibits modes with varying degrees of localization ranging from a free-sliding mode to quasiextended and localized modes. Succinct explanations of the origin of key features such as dispersionless modes, quasigaps, quasizone centers, and zone folding are also provided.
[S0163-1829(97)14717-8]

I. INTRODUCTION

Helium-atom scattering experiments reveal many new and interesting characteristics in the surface phonon dispersion curves of incommensurate overlayer/substrate systems which are not well understood.[1–3] In particular, the existence of dispersionless phonon branches is still an outstanding issue. Very recently, the phonon dispersion of Bi-O(001) surface of the high-T_c compound $Bi_2Sr_2CaCu_2O_8$ has been reported.[4] The surface was found to exhibit an incommensurate structure along the $\langle 110\rangle$ direction and a commensurate structure along the $\langle 110\rangle$ direction. Hence the phonon dispersion measured along the $\langle 110\rangle$ direction will exhibit the characteristics of a one-dimensional (1D) incommensurate system. The availability of the wealth of new experimental results has prompted us to study the vibrational dynamics of the one-dimensional incommensurate system as described by the infinite Frenkel-Kontorova (FK) chain.[5] Theoretical attempts to understand the vibrational dynamics of the incommensurate phase of the FK chain have used diverse approaches and approximations.[6–10] Although these treatments have reproduced some of the features observed in the experimental phonon dispersion curves,[1–3] none of them can capture all of the characteristic features of an incommensurate system such as the Goldstone (or free-sliding) mode, phason (dispersionless) modes, quasigaps, quasizone centers, zone folding, etc. In the continuum version of the FK model, Goldstone mode was obtained, but all other characteristic features of an incommensurate system are absent from the phonon dispersion curve.[6] Using a high-order commensurate structure, the Goldstone mode is usually absent.[10] Furthermore, dispersionless modes (phasons), which are the most striking features in the experimental phonon dispersion curves, are inherently absent in many of the previous theoretical approaches.[6–8,10] A molecular dynamics study of the FK chain exhibits the Goldstone mode, zone folding, dispersionless modes, etc.[9] However, this dispersionless mode is found to appear in the middle of the gap and has been interpreted as an edge-localized mode associated with the finite length of the chain. The origin of this mode is different from the dispersionless phason modes which appear in the vicinity of quasigaps. The latter modes arise genuinely from the incommensurate nature of the system. The failure of the previous theoretical studies to predict all the observed lattice dynamical features may be traced to the complex frequency spectrum of an incommensurate system, exhibiting modes with varying degrees of localization from the free-sliding, quasiextended, to localized modes. Hence approximations of one kind may account for certain features, but will miss out on the others. A correct picture can emerge only if the true ground state of the infinite FK chain can be accurately determined and a proper treatment of the lattice dynamics of the incommensurate structure which lacks the translational invariance can be carried out. In the present paper, both these issues have been taken into account carefully.

There is a vast amount of literature on the determination of the ground-state structure of the infinite FK chain. The most commonly used approach makes use of the force equilibrium conditions to generate a nonlinear area-preserving map and then to compare numerically the energies of orbits of the map to distinguish the ground-state configuration from the metastable and unstable states.[11] The approach of Aubry and co-workers[8,12] uses the force equilibrium condition and some general properties of the FK chain to determine the ground-state structure. Unfortunately, no concrete ground state was constructed for the *incommensurate* phase of the *infinite* FK chain.[8,11] Griffiths and Chou,[13] realizing the complexity of the numerical determination of the ground-state structure using force equilibrium conditions, devised a method based on effective potentials. This method yields both the ground-state energy and the corresponding particle configurations without any ambiguity as to whether the resulting state is metastable or unstable. In their approach, the ground-state configuration was obtained from the solution of a nonlinear eigenvalue equation for which a numerical grid method was used.[14] Although this approach can, in principle, be applied to study the incommensurate ground state, Chou and Griffith had not attempted to deal with this case because of numerical challenges posed in the treatment of this situation (see Ref. 14 for a discussion on this point). The efficiency of their numerical procedure scales as N^2 where N is the size of the segment under consideration. Furthermore, the accuracy of the numerical grid method used to solve the nonlinear eigenvalue equation is of the order $1/N$. In view of

the N^2 scaling and how the accuracy depends on N, this approach, in our opinion, will not be sufficiently efficient for our purposes where the phonon dispersion curve of an incommensurate phase of the *infinite* FK chain is calculated numerically (see the discussion in the following paragraph).

In this paper we develop an algorithm that determines efficiently and reliably the incommensurate ground-state structure of an infinite FK chain and then employ the real-space Green's function technique to treat the lattice dynamics of this system. The calculation of the diagonal and off-diagonal elements of the Green's function in real space requires the setting up of recursive relations as outlined in Ref. 18 to obtain convergence on each one of its elements. The Fourier transform of the converged real-space Green's function elements yields the phonon dispersion curve [see Eq. (9)]. Both these steps require determining the optimum size of the system so that properties of interest of the infinite FK chain are converged. Therefore, an algorithm that determines efficiently the ground state of the incommensurate FK chain is a very crucial issue in our numerical calculation of the phonon dispersion curve. We have devised an optimization scheme where the computational effort of determining the energy per atom scales linearly with the length of the chain. Our procedure (i) employs both the force equilibrium condition and energy minimization, (ii) does not impose periodic boundary conditions, (iii) invokes the center-of-symmetry concept to reduce the number of parameters in the calculation, and (iv) uses special sets of criteria [Eqs. 6(a)–6(d)] to determine if the size of the system under consideration would mimic an infinite Frenkel-Kontorova chain in its incommensurate state. The average energy per atom is computed by allowing relaxation of atoms in the chain and for chains of increasing lengths where step (iv) is verified for different segment sizes. The limiting value of $E_{\min}$ represents the ground state of the incommensurate structure of the FK chain. Once the ground-state structure is determined, the lattice dynamics of the incommensurate structure of the FK chain is studied using the real-space Green's function (RSGF) method.[15]

II. GROUND-STATE CONFIGURATION OF THE INFINITE FK CHAIN

Consider the FK model where a chain of particles connected by springs with a stiffness constant k and the natural length a is placed in an external sine-Gordon potential $V(x)=V_0[1-\cos(2\pi x/b)]$ with a period b. The total potential energy $U_{\rm tot}$ of such a system is given by

$$U_{\rm tot}=\sum_i \left[\frac{k}{2}(x_{i+1}-x_i-a)^2+V(x_i)\right]. \tag{1}$$

For a given V_0, the force equilibrium conditions $\partial U_{\rm tot}/\partial x_i=0$ yield

$$2y_i-y_{i+1}-y_{i-1}+\alpha\sin(2\pi y_i)=0, \tag{2}$$

where $y_i=x_i/b$ and $\alpha=\pi V_0/kb^2$. This indicates that, if any two adjacent positions y_i and y_{i-1} are known numerically, the configuration of all the particles in this chain can be determined. Therefore, the problem of determining the ground-state configuration would require the use of a two-parameter search for the minimization of the total energy of the system, which is a N^2 procedure. The problem can be reduced to a much simpler one-parameter search by recognizing the existence of a center of symmetry (COS) for the infinite FK chain.[16] For an infinite chain, the COS may be either at the particle site or midway between two adjacent particles which may lie either at the minimum or maximum of the substrate potential. For the first scenario, if we denote the reference COS site by y_0, we have

$$y_1-y_0=y_0-y_{-1}. \tag{3}$$

Substituting Eq. (3) into Eq. (2), we obtain

$$\sin(2\pi y_0)=0.$$

Hence the COS can be either $y_0=0$ (a minimum point of the substrate potential) or $y_0=\frac{1}{2}$(a maximum point of the substrate potential). For the case where the COS is at the middle point between two adjacent sites labeled 0 and 1, respectively, we have

$$y_2-y_1=y_0-y_{-1}. \tag{4}$$

Equations (2) and (4) then lead to

$$\sin(2\pi y_1)=-\sin(2\pi y_0).$$

Therefore, in this case, either $y_1=-y_0$ or $y_1=-y_0+1$. The above consideration leads to four possible cases. By defining $y_1-y_0=a/b+\delta$, the four possible cases can be summarized as (i) $y_0=0$, $y_1=a/b+\delta$, (ii) $y_0=\frac{1}{2}$, $y_1=\frac{1}{2}+a/b+\delta$, (iii) $y_0=-\frac{1}{2}(a/b+\delta)$, $y_1=\frac{1}{2}(a/b+\delta)$, and (iv) $y_0=-\frac{1}{2}(a/b+\delta-1)$, $y_1=\frac{1}{2}(a/b+\delta+1)$, respectively. These relations reduce the numerical problem of determining the equilibrium particle positions of the ground-state configuration to a one-parameter search. The average energy per particle of the system is now a function of the parameter δ alone and is given by

$$E(\delta)=W\lim_{\epsilon\to 0}\frac{1}{n(\epsilon)}\sum_{i=1}^{n(\epsilon)}\left[\left(y_i-y_{i-1}-\frac{a}{b}\right)^2+\frac{\alpha}{\pi}[1-\cos(2\pi y_i)]\right], \tag{5}$$

where $W=\frac{1}{2}kb^2$. The calculation of the energy per particle, $E(\delta)$, is carried out for a series of n until the value of $E(\delta)$ has converged to the desired accuracy. We also ensure that the selected value of n would mimic an infinite incommensurate system by requiring that the environment of the particle n be similar (to the extent controlled by a parameter ϵ), but not identical to the reference particle labeled 0. Thus the optimum value of $n(\epsilon)$ is chosen based on the following sets of conditions:

$$|y_n-j-y_0|\leq\epsilon, \tag{6a}$$

$$|(y_n-y_{n-1})-(y_0-y_{-1})|\leq\epsilon, \tag{6b}$$

$$|(y_{n+1}-y_n)-(y_1-y_0)|\leq\epsilon, \tag{6c}$$

and

$$|y_n-j|<1, \tag{6d}$$

where j is an integer identifying the substrate potential well in which the particle n resides and ϵ is a small number, but not equal to zero. We found that, using this algorithm,

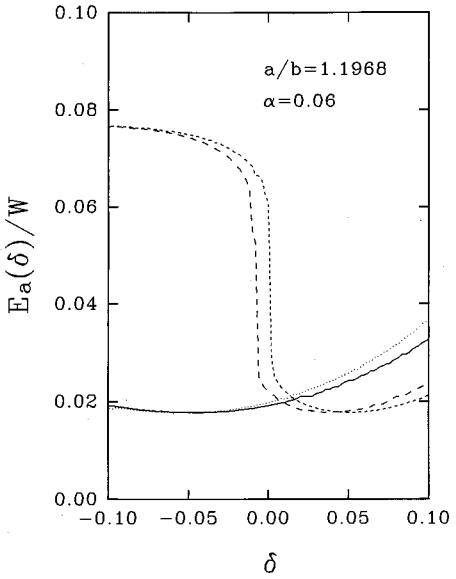

FIG. 1. Average energy per particle (normalized by W) vs the relaxation displacement, δ, for the parameter set $a/b=1.1968$ and $\alpha=0.06$. Results are shown for different choices of the COS where solid, long-dashed, short-dashed, and dotted lines correspond to cases (i)–(iv) as described in the text.

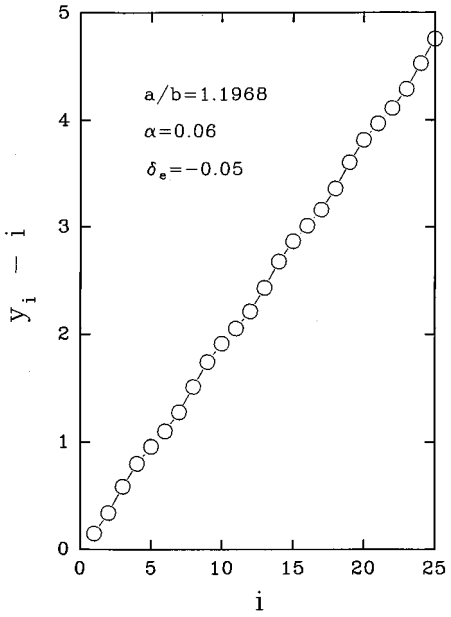

FIG. 2. Relative position of the ith particle of the chain with respect to the minimum of the ith substrate potential well is shown for different particles sites on the chain.

$E(\delta)$ is converged to the same order as ϵ and the optimum value of n is linked to the parameter ϵ. For example, choosing $\epsilon\sim10^{-5}$, one finds the optimum number of particles in the chain to be $n\sim1773$, while $\epsilon\sim10^{-12}$ requires $n\sim3477$ for the incommensurate system under study ($a/b=1.1968$ and $\alpha=0.06$). The energy per particle is then calculated for different values of δ, and the minimum value of E determines the ground-state configuration. We also performed this calculation for the four different choices of y_0 and y_1 as outlined earlier. The results are shown in Fig. 1. Although the relaxation process is different in the above four cases, all of them yield the same minimum value of energy. This can be understood on the basis of the free-sliding behavior of the incommensurate phase. Therefore, in the calculation presented below, we chose to proceed with the case where the COS is at a particle site and at the minimum of the substrate potential.

The ground-state structure of the infinite FK chain is controlled by the interplay of two factors: the mismatch a/b and the parameter α. In our calculation, since we allow for the relaxation of the elastic chain on the substrate to determine the ground-state configuration, no matter whether a/b is a rational or irrational number, it only determines one aspect of the initial state (with the other part given by α). The final ground state is approached by the relaxation of the particles in the combined field of the elastic potential and the substrate potential. Hence the value of the mismatch a/b *alone* has no direct bearing on the eventual outcome (commensurate or incommensurate) of the final ground-state structure. We have studied the ground-state structure for $a/b=1.1968$ and a series of values of α by minimizing E with respect to δ. For the incommensurate structure, the E vs δ curve has a very broad minimum, whereas for a high-order commensurate structure this curve has a sharp global minimum. We found that there is a transition from an incommensurate ground state to a very-high-order commensurate ground state for $\alpha=0.23$ (with a commensurability period of $514a$ for $\epsilon=10^{-21}$). In general, for a given natural mismatch a/b, α is the factor which determines the nature of the ground-state structure. When α is small, one may obtain an incommensurate phase as the ground state, whereas when α is sufficiently large, a high-order commensurate phase may be obtained as the ground state. It should be remarked that many of the previous works[10,12] which do not allow for the relaxation of atoms in the chain assume right at the outset $\overline{a/b}$ to be an irrational number, where $\overline{a}$ is the *average periodicity* of the chain. In our calculation, we allow for the relaxation and determine explicitly whether a given set of parameters α and a/b, where a is the *natural periodicity* of the chain, would lead to an incommensurate structure. Since the parameter set $a/b=1.1968$ and $\alpha=0.06$ was found to yield an incommensurate ground-state structure, in what follows we shall use this set of parameters to investigate the properties of the incommensurate state of the FK chain.

An examination of the particle separation of the relaxed ground-state structure relative to the initial particle separation in the FK chain reveals a ''quasiperiodic behavior'' with the amplitude of interparticle expansions or contractions varying from site to site ($y_i-y_{i-1}-a/b$ vs i). One can define an average periodicity for the structure by checking the distribution of distances between each pair of adjacent maximum expansions or contractions. We found that approximately 70% of them are separated by a distance $\sim5a$ and that 30% of them are apart by a distance $\sim6a$. From this we concluded that the average periodicity of the incommensurate system under study ($a/b=1.1968$, $\alpha=0.06$) is $5.33a$ (or, equivalently, $6.38b$). This result is also substantiated by a plot of y_i-i vs i as shown in Fig. 2, where the ordinate represents the particle distance from the minimum of the ith substrate potential. This figure reveals a quasiperiodic soliton structure, where the length of an overlayer soliton is seen to be approximately $5a$.

III. LATTICE DYNAMICS OF THE FK CHAIN

In this section, we discuss the results of our lattice dynamical study of the incommensurate ground state structure of a FK chain. To calculate the phonon density of states and eigenvectors, we have used the method of real-space Green's functions as developed in Refs. 17–19. Using this method, one can obtain exact expressions for the diagonal and off-diagonal elements of the Green's function regardless of the dimensions of the system (1D or 3D) as long as the range interaction of the system is finite. The eigenvector calculation from this method is described in Ref. 20. It has been shown that this method yields correct local symmetry even for the degenerate modes. The RSGF method has been shown to be successful in the treatment of dynamics of systems with reduced symmetry such as surfaces, fractals, defects, etc.[15]

Several other methods are available[21–23] which may be used to determine the real-space Green's function of a one-dimensional Frenkel-Kontorova system. Since our intention is to study eventually a 2D Frenkel-Kontorova model and other real incommensurate materials, we have adopted the method developed in Refs. 17–19. Furthermore, in one of our earlier works,[18] a detailed comparison of the technique used in Ref. 23 and our method has been presented.

For the incommensurate system under study, since interactions are restricted to first-nearest neighbors, the force constant matrix H of the system reduces to a simple tridiagonal matrix where the diagonal elements $\mathbf{h}_{ll}=2(k/\mu)[1+\pi\alpha\cos(2\pi\overline{y_l})]$ and the off-diagonal elements $v_{l,l+1}=v_{l,l-1}=-k/\mu$ are all scalars. Here $\overline{y_l}$ is the position of the lth particle in the ground state and μ is the mass of the particle in the overlayer. The Green's function operator for the matrix H is defined by

$$G=[(\varpi^2+i\eta)I-H]^{-1}, \tag{7}$$

and the corresponding local density of vibrational states is given by

$$\rho_l(\varpi^2)=-\frac{1}{\pi}\lim_{\eta\to 0}\ \mathrm{Im}\ \mathrm{Tr}[G_{ll}(\varpi^2+i\eta)], \tag{8}$$

where the diagonal element G_{ll} is the local Green's function. As mentioned earlier, an exact method for calculating G_{ll} can be found in Refs. 17–19.

Using Eq. (8), the local phonon density of states (LDOS) for the incommensurate structure corresponding to the case $a/b=1.1968$ and $\alpha=0.06$ has been calculated. The results for sites from $i=0$ to $i=4$ (about one soliton structure) and from $i=5$ to $i=9$ (second soliton) are shown in Figs. 3(a) and 3(b), respectively. One can see that, for a five-particle soliton superlattice overlayer, the local densities of states split off into five parts, and the largest gap occurs in the low-energy region. The local phonon density of states varies from a given site to the next site. Furthermore, the LDOS for the two soliton structures are similar [compare Fig. 3(a) with Fig. 3(b)], but a careful examination reveals that they are not identical. One consequence of this result is that when one examines the total phonon density states for the system, one obtains smeared gaps. This result is in contrast to the case of the commensurate system where the gaps of phonon spectrum are clearly defined. The most interesting features are the low-energy parts of the local density of states. It begins from zero frequency and does not exhibit any gap near zero frequency. This clearly indicates the existence of the Goldstone mode (zero frequency) which is responsible for the free sliding of the incommensurate chain over the substrate. Furthermore, the LDOS in the $\omega\to 0$ regime is smaller for a particle close to the minima of the substrate potential compared to the maxima of the substrate potential. This means that the particle close to the minima of the potential is less free to move compared to others.

In order to compare our results with experiments which typically have phonon frequencies as functions of the wave vector, it is necessary to consider the Green's function in the ''quasi-wave vector'' space (q). The Green's function in the quasi-wave-vector space, $G_q^{(n)}(\varpi^2+i\eta)$, is obtained via the Fourier transform of $G_{ll'}^{(n)}(\varpi^2+i\eta)$, i.e.,

$$G_q^{(n)}(\varpi^2+i\eta)=\frac{1}{n}\sum_{l,l'}\ G_{ll'}^{(n)}(\varpi^2+i\eta)e^{iqR_{ll'}}. \tag{9}$$

The corresponding phonon density of states in q space is given by

$$\rho(q,\varpi^2)=-\frac{1}{\pi}\lim_{n\to\infty}\lim_{\eta\to 0}\ \mathrm{Im}[G_q^{(n)}(\varpi^2+i\eta)]. \tag{10}$$

It should be commented that in order to compute accurately and efficiently the phonon density of states, care must be taken that the Fourier transform of the real-space Green's function matrix, which involves a double summation over all the sites in the FK chain, is converged. This in turn requires that all the elements of the Green's function in real space are converged to the desired accuracy (see Ref. 18), where the convergence is tested by enlarging the size of the FK chain. Furthermore, when the system is enlarged, we ensure that the FK chain remains in the incommensurate state and that the optimum size of the chain satisfies Eqs. (6a)–(6d).

The phonon dispersion relation for the incommensurate structure of an infinite FK chain has been obtained by projecting $\rho(q,\varpi)$ onto the $\varpi-q$ plane, where $\rho(q,\varpi)=2\varpi\ \rho(q,\varpi^2)$. The results are shown in Figs. 4(a)–4(c) for different parameter sets. The dispersion curve corresponding to the parameter set $a/b=1.1968$ and $\alpha=0.06$ is shown in Fig. 4(a). It reveals many interesting features: (i) The dispersion curve has a zero-frequency (Goldstone) mode, characterizing the free sliding of the incommensurate chain over the substrate. This mode will not be present for a commensurate structure including a high-order commensurate structure[10] or when a periodic boundary condition is used to mimic an infinite FK chain. (ii) The main branch is folded and the main quasigap can be seen at a wave vector which is related to the average periodicity of the incommensurate overlayer (i.e., $q_{\mathrm{gap}}=\pi/\overline{a}$, where $\overline{a}=5.33a$ or $6.38b$). In Fig. 4(a) this feature is observed at $q=0.0784$, where the wave vector is expressed in the reduced unit of $2\pi/b$. The zone folding and the appearance of the quasigap at this value of the wave vector are an indication of the struggle of the system to find a compromise between the incommensurate nature of the system and the average periodicity. It should be noted that for a high-order commensurate structure, the zone folding observed will be related to the commensurability pe-

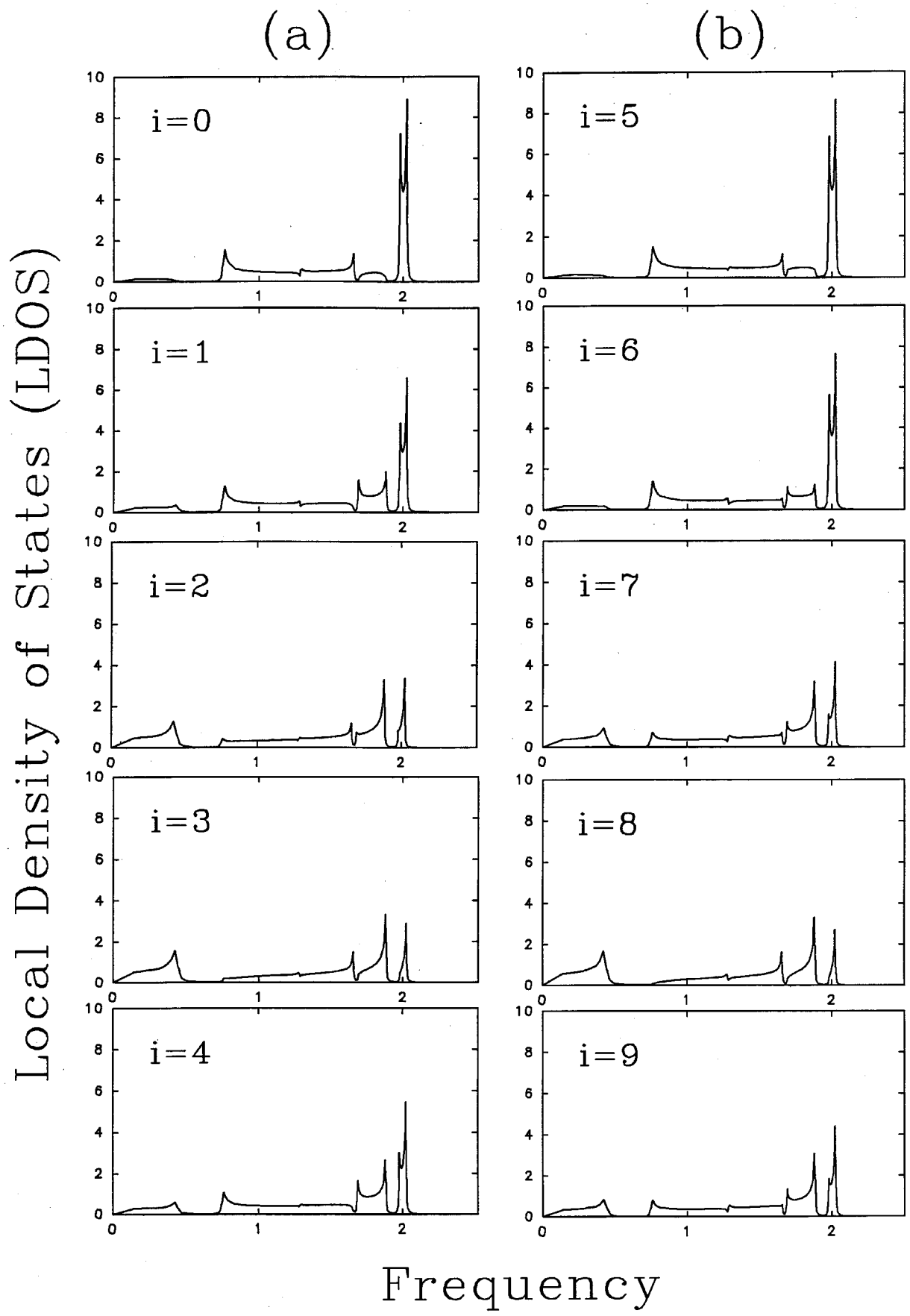

FIG. 3. (a) Local phonon density of states for particles at sites from $i=0$ to $i=4$; (b) LDOS from $i=5$ to $i=9$. Both results correspond to the parameter set $a/b=1.1968$ and $\alpha=0.06$.

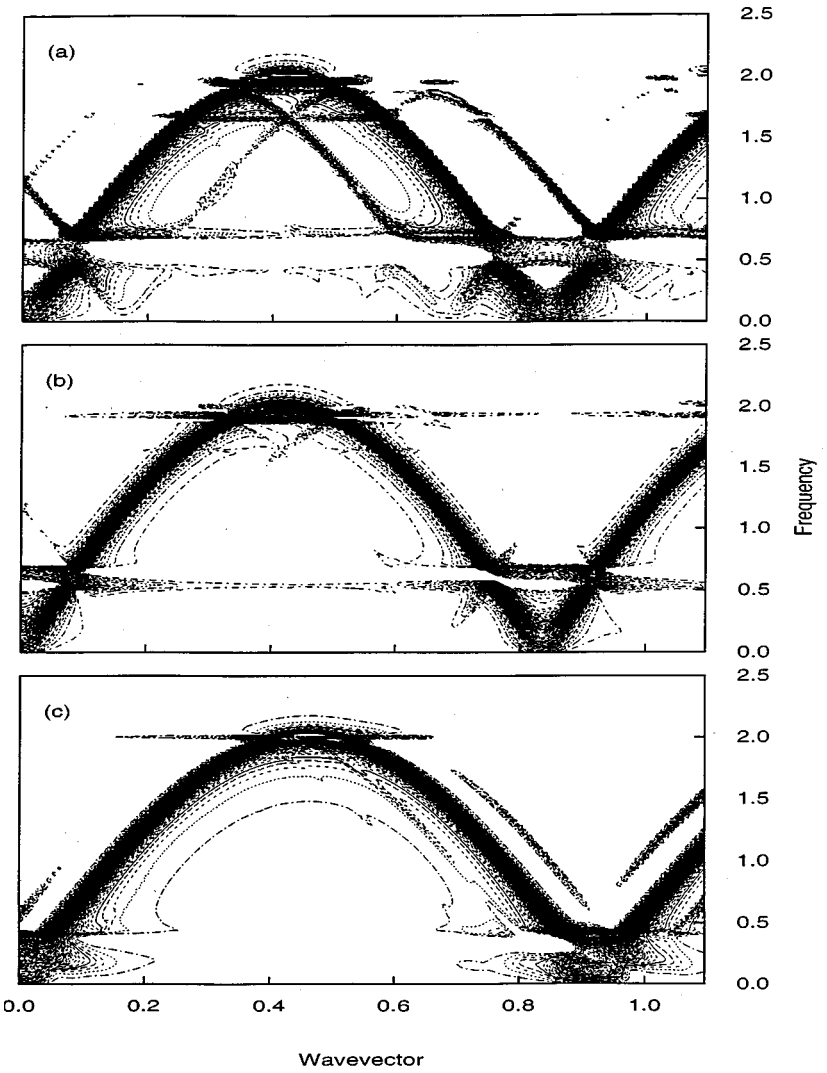

FIG. 4. Phonon dispersion curves corresponding to different incommensurate structures of the infinite FK chain: (a) $a/b=1.1968$ and $\alpha=0.06$, (b) $a/b=1.1968$ and $\alpha=0.03$, and (c) $a/b=1.0968$ and $\alpha=0.025$. The quasi-wavevector and the frequency are normalized by $2\pi/b$ and $\sqrt{k/\mu}$, respectively. The main quasigap in (a) occurs at $q\simeq 0.0784$ and the quasizone center occurs at $q\simeq 0.157$.

riod of the system. (iii) In Fig. 4(a), the zone boundaries are not clearly defined because of the lack of a well-defined periodicity of the system. (iv) One also finds in Fig. 4(a) a quasizone center at a wave vector which is approximately twice the value of the wave vector at which the gap occurs (i.e., $q_{\text{zone center}}\simeq 2\pi/\overline{a}=0.157$). Associated with this quasizone center, a subsidiary branch running parallel to the main branch can be seen. This branch has a weaker intensity compared to the main branch. (v) Finally, the most striking feature is the presence of a pair of dispersionless modes running just above and beneath the main quasigap at $\varpi=0.42$ and $\varpi=0.76$ [see Fig. 4(a)], respectively. Other such pairs of dispersionless modes associated with quasigaps at higher frequencies [e.g., at $\varpi=1.65$ and $\varpi=1.69$ in Fig. 4(a)] can also be seen, but they all have weaker intensities. There are a number of interesting properties associated with these pairs of dispersionless modes. We first start with a caveat. Although the dispersionless mode has the same frequency for different values of q, it cannot be assumed to be degenerate. This is due to the fact that q cannot be used to designate the states of an incommensurate structure as it lacks the translational invariance. To test this scenario, a careful analysis of the eigenvectors corresponding to dispersionless modes was carried out using the RSGF method. It has been shown that if the columns of Im G are either identical or differ by only a multiplication factor, the mode in question is of nondegenerate nature.[20] Using this method, the dispersionless modes were found to be indeed nondegenerate. These modes appear as flat modes in the dispersion curve simply because they can be expressed as linear combinations of plane-wave states designated by q. The eigenvectors corresponding to the pair of low-frequency dispersionless modes associated with $\varpi=0.42$ and $\varpi=0.76$ are shown in Figs. 5(a) and 5(b), respectively. First, it can be seen that these dispersionless modes are very localized in real space, while they appear very extended in q space [see Fig. 4(a)]. When the particle displacements are examined carefully (see the insets), it can be found that all particles in a given soliton structure (approximately five sites in the present case) move in unison. Hence these modes may be termed as ''acoustic phasons.'' It can also be seen from the insets that the phase of the soliton gets repeated over a distance that is shorter for the mode at $\varpi=0.76$ as compared to the mode at $\varpi=0.42$. It is also found that the center of gravity of the displacement pattern in both cases is located around the site $i=0$. Thus these modes are not likely to be excited by optical waves. The eigenvectors corresponding to the pair of high-frequency dispersionless modes at $\varpi=1.65$ and $\varpi=1.69$ are shown in Figs. 6(a) and 6(b), respectively. Unlike the acoustic phason modes, in this case particles in the same soliton structure do not move

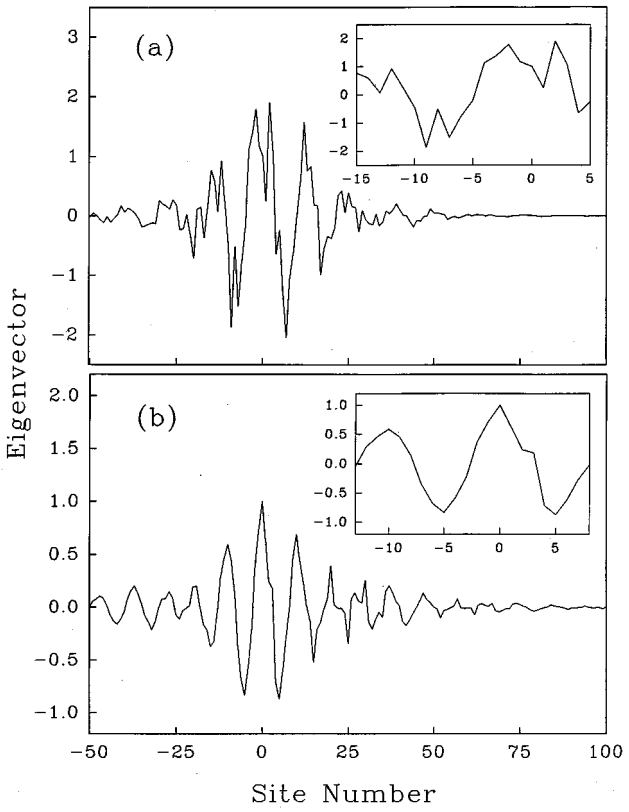

FIG. 5. Eigenvectors corresponding to the dispersionless acoustic phason modes at (a) $\varpi = 0.42$ and (b) $\varpi = 0.76$, respectively.

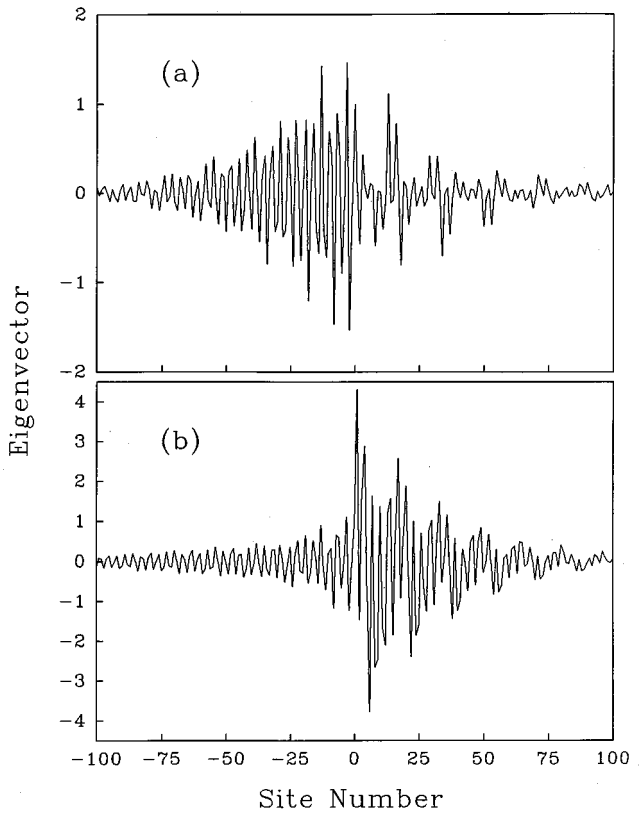

FIG. 6. Eigenvectors corresponding to the dispersionless optical phason modes at (a) $\varpi = 1.65$ and (b) $\varpi = 1.69$, respectively.

in unison and hence they will be termed as ''optic phasons.'' These modes are found to be more extended in real space as compared to the acoustic phasons, and accordingly their extension in the q space is shorter than that of the acoustic phasons [see Fig. 4(a)]. The centers of gravity of the displacement pattern of the optic phasons at $\varpi = 1.65$ and $\varpi = 1.69$ are located at $i \neq 0$ and in fact are on the opposite sides of the central site at $i = 0$. Hence these modes are likely to be excited by optical waves.

We have also examined the width of the quasigap as a function of the parameters defining the system and found that it decreases with the decreasing value of the parameter α [compare Fig. 4(a) with Fig. 4(b)]. We also found that separation between the main branch and the subsidiary branch depends on the ratio of the mismatch, a/b. It decreases with the decreasing value of the mismatch ratio [compare Figs. 4(a) and 4(c), respectively]. From Fig. 4(b), it can be seen that, as the main quasigap becomes sufficiently narrow (for sufficiently small α), the pair of dispersionless modes associated with the gap starts to merge into one. This situation was actually observed in experiments.[2–3] Figure 4(c) shows that the extension of the main dispersionless mode in the q space is much shorter compared to the corresponding modes in Figs. 4(a) and 4(b). Hence this mode is more extended in real space, which is a reflection of the fact that the size of the soliton for $a/b = 1.0968$ is larger compared to the case when $a/b = 1.1968$.

IV. CONCLUSION

In this work, both the ground-state structure and the lattice dynamics of an infinite Frenkel-Kontorova chain in its incommensurate state have been reported. The algorithm to determine the ground state uses force equilibrium conditions, energy minimization, and the center-of-symmetry concept. To mimic an infinite system, we used a convergence scheme which circumvents the use of periodic boundary conditions or a supercell approach, thereby eliminating the possibility of obtaining a high-order commensurate structure. The main highlights of our lattice dynamical calculations are as follows: The dispersionless modes have been obtained in a theoretical calculation of the lattice dynamics of the FK chain. Both acousticlike and opticlike phason modes have been identified. Contrary to ones's intuition, the dispersionless modes have been identified as nondegenerate modes by the eigenvector analysis. In addition, all the signature features such as Goldstone modes, quasigaps, zone folding, quasizone centers, etc., have been obtained in our study. In our opinion, this work provides a complete, coherent, and consistent picture of the lattice dynamics of a one-dimensional incommensurate system as described by the Frenkel-Kontorova model.

ACKNOWLEDGMENTS

This research was supported by the National Science Foundation through Grant Nos. EHR-9108764 and OSR-9452895. C.S.J. would also like to acknowledge the support from the Cottrell College Science Award of Research Corporation.

[1] R. B. Doak and D. B. Nguyen, Phys. Rev. B **40**, 1495 (1989).
[2] G. Benedek, J. Ellis, A. Reichmuth, P. Ruggerone, H. Scheif, and J. P. Toennies, Phys. Rev. Lett. **69**, 2951 (1992).
[3] S. A. Safron, G. G. Bishop, J. Duan, E. S. Gillman, J. G. Skofronick, N. S. Luo, and P. Ruggerone, J. Phys. Chem. **97**, 2270 (1993).
[4] U. Paltzer, D. Schmicker, F. W. de Wette, U. Schroeder, and J. P. Toennies (unpublished).
[5] T. A. Kontorova and Ya. I. Frenkel, Zh. Eksp. Teor. **8**, 89 (1938).
[6] W. L. McMillan, Phys. Rev. B **16**, 4655 (1977).
[7] A. D. Novaco, Phys. Rev. B **22**, 1645 (1980).
[8] M. Peyrad and S. Aubry, J. Phys. C **16**, 1593 (1983).
[9] K. M. Martini, S. Burdick, M. El-Batanouny, and G. Kirczenow, Phys. Rev. B **30**, 492 (1984).
[10] J. E. Black and D. L. Mills, Phys. Rev. B **42**, 5610 (1990).
[11] W. Selke, in *Phase Transitions and Critical Phenomena*, edited by C. Domb and J. L. Lebowitz (Academic, London, 1992), Vol. 15, p. 1.
[12] S. Aubry, Physica D **7**, 240 (1983); J. Phys. C **16**, 2497 (1983); J. Phys. (Paris) **44**, 147 (1983); S. Aubry and P. Y. Le Daeron, Physica D **8**, 381 (1983); L. de Seze and S. Aubry, J. Phys. C **17**, 389 (1984).
[13] R. B. Griffiths and W. Chou, Phys. Rev. Lett. **56**, 1929 (1986).
[14] W. Chou and R. B. Griffiths, Phys. Rev. B **34**, 6219 (1986).
[15] See, S. Y. Wu and C. S. Jayanthi, Int. J. Mod. Phys. B **9**, 1869 (1995), and references therein.
[16] J. E. Sacco and J. B. Sokoloff, Phys. Rev. B **18**, 6549 (1978); Sacco and Sokoloff imposed a *periodic boundary condition* and then invoked the existence of the COS for the *periodic* chain to simplify the calculation. Their procedure is expected to lead to a particular class of high-order commensurate structure.
[17] K. S. Dy, S. Y. Wu, and T. Spratlin, Phys. Rev. B **20**, 4237 (1979).
[18] S. Y. Wu, J. A. Cocks, and C. S. Jayanthi, Phys. Rev. B **49**, 7957 (1994).
[19] S. Y. Wu, J. A. Cocks, and C. S. Jayanthi, Comput. Phys. Commun. **71**, 125 (1992).
[20] C. S. Jayanthi, S. Y. Wu, and J. A. Cocks, Phys. Rev. Lett. **69**, 1955 (1992).
[21] A. Mackinnon, J. Phys. C **13**, L1031 (1980).
[22] P. A. Lee and D. S. Fisher, Phys. Rev. Lett. **47**, 882 (1981).
[23] R. Haydock, V. Heine, and M. J. Kelly, J. Phys. C **5**, 2845 (1972).